physica **pss** status solidi **b**
www.pss-b.com

basic solid state physics

The magnetoelectric effect and double-perovskite structure

Safa Golrokh Bahoosh[1], Julia M. Wesselinowa[2], and Steffen Trimper*[,3]

[1] Max Planck Institute of Microstructure Physics, Weinberg 2, 06120 Halle, Germany
[2] Department of Physics, University of Sofia, Bldvd. J. Bouchier 5, 1164 Sofia, Bulgaria
[3] Institute of Physics, Martin-Luther-University, Von-Seckendorff-Platz 1, 06120 Halle, Germany

* Corresponding author: e-mail **steffen.trimper@physik.uni-halle.de**, Phone: +49 345 55 25432, Fax: +49 345 55 25446

Based on a microscopic model with a biquadratic magneto-electric coupling the properties of Bi_2NiMnO_6 thin films are investigated. Using Green's functions the phonon spectrum is calculated which is determined by the polarization and the magnetization. The phonon energy and its damping offer a kink at the magnetic phase transition temperature. The phonon energy is enhanced if an external magnetic field is increased, whereas, the damping of the phonons decreases. The observed behavior is a strong evidence for a magnetoelectric coupling. The relevance of our approach for other multiferroics is discussed.

© 2012 WILEY-VCH Verlag GmbH & Co. KGaA, Weinheim

1 Introduction Multiferroics, defined as materials with coexistence of at least two of the electric, elastic and magnetic orders, have attracted enormous research activities recently. They are of interest for memory and logic device applications, because the coupling between ferroelectric and magnetic properties enables a dynamical interaction between the corresponding order parameters. As a new development double-perovskite multiferroic compounds of the form $A_2BB'O_6$ have been theoretically and experimentally designed. To this group of material belongs for instance Bi_2NiMnO_6 (BNMO), Bi_2FeMnO_6 (BFMO), Bi_2CoMnO_6 (BCMO), and Bi_2FeCrO_6 (BFCO). Especially in BMNO the Bi^{3+} ion, located at the A site in the perovskite structure, gives rise to a structural distortion at $T_c = 485$ K which leads to ferroelectricity. On the other hand the B- and B'-site ordering of the Ni^{2+} and Mn^{4+} ions, respectively, in a rock-salt configuration gives rise to a ferromagnetic behavior at the lower critical temperature $T_N = 140$ K) [1]. Further experimental studies of BNMO thin films have confirmed the strong coupling between magnetic and ferroelectric phases [2–4]. Other studies of multiferroic Bi_2FeCrO_6 (BFCO) thin films have offered a similar behavior [5–7]. The first density functional studies for BNMO and Y_2NiMnO_6 (YNMO) have been presented in Ref. [8] and more recently in Ref. [9]. Temperature-dependent Raman measurements in BNMO thin films [10] reveal a softening below 140 K and a step-like anomaly in between 420 and 490 K of the main Raman peak frequency. This observation provides a strong evidence for the multiferroic behavior of the material. Furthermore, the results for thin films are similar to those of bulk materials. Infrared reflectance spectra of Bi_2FeCrO_6 thin films, reported in Ref. [11], yields similar results. One observes some phonon anomalies near to the phase transition.

In spite of sufficient experimental findings a well motivated microscopic model describing the situation is still missing. The present paper is focused on the spin–phonon coupling. We demonstrate that such a coupling is quite relevant in the double perovskite structure. In particular, the influence of the magnetoelectric coupling on phonon excitation and its damping is analyzed.

2 Magnetoelectric coupling We propose the following Hamiltonian for the materials characterized above:

$$H = H^e + H^m + H^{me} + H^p. \tag{1}$$

Here H^e is the electric part and H^m is the magnetic contribution. The magnetoelectric coupling is described by H^{me} and the phonon interaction and the related spin–phonon coupling are included in H^p.

TH-2012-57

Phys. Status Solidi B 249, No. 8 (2012) 1603

Original

Paper

2.1 Ferroelectric and magnetic interaction The electric part H^e is given by the transverse Ising model:

$$H^e = -\Omega \sum_i S_i^x - \frac{1}{2} \sum_{ij} J_{ij} S_i^z S_j^z, \tag{2}$$

where S_i^x, S_i^z are the spin-1/2 operators of the pseudo-spins. The operator S^z describes the positions of the Bi-ions in a double well potential and S^x plays the role of the kinetic energy. The parameter $J_{ij} > 0$ denotes the nearest-neighbor pseudo-spin interaction and Ω is the tunneling frequency. Surface effects can be included by different coupling parameters for the free surface shells, denoted by $\Omega^{(s)}$ and $J^{(s)}$, respectively. The related parameters for the bulk are written as $\Omega^{(b)}$ and $J^{(b)}$. Regarding the surface effects and the discussion on the influence of spin–phonon coupling, see below, let us mention that the exchange coupling $J_{ij} \equiv J(\boldsymbol{r}_i - \boldsymbol{r}_j)$ depends on the real distance between the spins and consequently on the lattice parameter, the symmetry of the lattice and the numbers of nearest neighbors. The larger the distance of the spins the weaker is the interaction. This fact will be incorporated in the microscopic model by the spin–phonon coupling. For more technical reasons the model in Eq. (2) is considered in a rotated frame in the x–z-plane with an angle θ which is determined by the minimum of the ground state energy.

Before we proceed let us comment the applicability of the transverse Ising model for ferroelectrics. Originally the model had been proposed by Blinc and de Gennes, see Ref. [12], to describe order–disorder ferroelectrics with the prototype KDP. In such H-bonded ferroelectrics the transverse field represents the tunneling frequency of the proton between two equilibrium positions within the H bonds. In case the tunneling frequency Ω is very small compared to the interaction constant J one may use the Hamiltonian in Eq. (2) for such order–disorder material as for instance $NaNO_2$ and TGS, where the tunneling is negligible. The Ising model in a transverse field is also successfully applied for so-called displacive type ferroelectrics such as $BaTiO_3$ (BTO) and BTO thin films [13–15]. According to the order–disorder model, the disorder in the paraelectric phase of BTO is associated with the position of the Ti ions. Instead of occupying the body center positions as in an ideal cubic perovskite structure the Ti ions are randomly displaced along the cube diagonals. This effect causes the disorder which had been observed in the vibration spectrum of BTO single crystal as a function of temperature by Raman and infrared measurements [16]. The results suggest that the transverse Ising model should be applicable to all types of ferroelectrics.

The magnetic subsystem is characterized by the Heisenberg Hamiltonian H^m written in the form

$$H^m = -\frac{1}{2} \sum_{ij} A_{ij} \boldsymbol{B}_i \cdot \boldsymbol{B}_j - h \sum_i S_i^z. \tag{3}$$

Here $\boldsymbol{B}_i$ is the Heisenberg spin operator and the exchange integral A_{ij} represents the coupling between the magnetic Ni^{2+}- and Mn^{4+}-ions at the B- and B'-sites i and j, respectively. The external magnetic field is denoted as $h \equiv g\mu_B H$.

2.2 Magnetoelectric and spin–phonon coupling The term H^{me} in Eq. (1) describes the coupling between the magnetic and the electric subsystems in the ferroic compound. Despite the great effort in understanding the magnetoelectric effects the form of the magnetoelectric coupling and the underlying mechanism is still an important issue for debate. Let us notice that, for example, orthorhombic perovskite $RMnO_3$ and hexagonal $RMnO_3$ belong to different classes of magnetoelectrics. In our paper we use the Ising model in a transverse field and a biquadratic coupling between the pseudo-spins and magnetic moments, see Eq. (4) implies that the magnetic and the ferroelectric subsystems are subjected to independent ordering mechanism which is manifested by well separated transition temperatures $T_c \gg T_N$. So the biquadratic coupling is relevant for hexagonal $RMnO_3$ [17] and BFO [18]. In the orthorhombic perovskite $RMnO_3$ the leading magnetoelectric interaction term is linear in the electric dipole moment due to the improper nature of its ferroelectricity [19]. A similar situation is realized in RMn_2O_5, which is an improper ferroelectric system, too. Because BNMO offers a great difference between the two critical temperature we suggest likewise a biquadratic magnetoelectric coupling between the two order parameters:

$$H^{me} = -g \sum_{<klij>} S_k^z S_l^z \boldsymbol{B}_i \cdot \boldsymbol{B}_j. \tag{4}$$

Here g is the coupling constant between the magnetic and the electric order parameters.

There is an evidence for a strong spin–lattice coupling in the double-perovskite multiferroics [10, 11, 20], therefore, the total Hamiltonian is supplemented by the additional part

$$H^p = H^{p0} + H^{sp} \tag{5}$$

representing the phonon part. Here, H^{p0} describes the lattice vibrations in terms of the normal coordinates Q_i and the related frequency ω_{i0}. In order to stabilize the distorted phase below T_c anharmonic terms of third and fourth order have to be included

$$H^{p0} = \frac{1}{2!} \sum_{ij} \omega_{0i} \omega_{0j} Q_i Q_j + \frac{1}{3!} \sum_{ijr} B_{ijk}^p Q_i Q_j Q_r$$

$$+ \frac{1}{4!} \sum A_{ijrs}^p Q_i Q_j Q_r Q_s. \tag{6}$$

So the electric part of our model includes both order–disorder-like elements manifested by the pseudo-spin Hamiltonian in Eq. (2) and displacive-like elements to be contained in Eq. (6). The normal coordinate Q_i can be expressed in terms of phonon creation and annihilation

operators according to

$$Q_i = (2\omega_{0i})^{-1/2}(a_i + a_i^+). \tag{7}$$

The remaining contribution H^{sp} comprises the coupling between the pseudo-spins of the ferroelectric subsystem and of the magnetic spins with the phonons. This spin–phonon coupling reads:

$$H^{\mathrm{sp}} = -\frac{1}{2}\sum \left(\overline{F}_{ij}^{\mathrm{e}} Q_i S_j^z - \frac{1}{2}\overline{R}_{ijr}^{\mathrm{e}} Q_i Q_j S_r^z \right)$$
$$-\frac{1}{2}\sum \left(\overline{F}_{ij}^{\mathrm{m}} Q_i B_j^z - \frac{1}{2}\overline{R}_{ijr}^{\mathrm{m}} Q_i Q_j B_r^z \right), \tag{8}$$

where the superscript e and m are related to the electric and magnetic subsystems, respectively. $F(i) = \overline{F}(i)/(2\omega_{0i})^{1/2}$ and $R(i,j) = \overline{R}(i,j)/(2\omega_{0i})^{1/2}(2\omega_{0j})^{1/2}$ designate the amplitudes for coupling phonons to the spin excitations in first and second order.

3 Phonon spectrum

The complete system is analyzed by retarded Green's functions. Especially the phonon part is studied with the following function defined by

$$g_{ij}(t) = \left\langle\left\langle a_i(t); a_j^\dagger(0) \right\rangle\right\rangle$$
$$= -i\Theta(t - t')\langle [a_i(t), a_j^\dagger]\rangle. \tag{9}$$

The two-dimensional Fourier transform $g_{n_i n_j}(\boldsymbol{k}_\parallel, \omega)$ has the following form:

$$g_{ij}(\omega) = \frac{1}{N'}\sum_{\boldsymbol{k}_\parallel} \exp(i\boldsymbol{k}_\parallel(\boldsymbol{r}_i - \boldsymbol{r}_j))g_{n_i n_j}(\boldsymbol{k}_\parallel, \omega), \tag{10}$$

where N' is the number of sites in any of the lattice planes. Whereas, $\boldsymbol{r}_i$ represents the position vectors of site i, the quantity $n = 1, N$ denotes the layer ordering number beginning with one surface ($n = 1$) and terminating at the other one ($n = N$). The vector $\boldsymbol{k}_\parallel = (k_x, k_y)$ is a two-dimensional wave vector parallel to the surface. The summation is taken over the Brillouin zone.

For the approximate calculation of the phonon Green's function we follow the line proposed in Ref. [21]. The phonon energy spectrum is

$$\frac{\omega^2(\boldsymbol{k}_\parallel)}{\omega_0} = \omega_0 - 2(1/2\,P^2\cos\theta R^e(\boldsymbol{k}_\parallel) + M^2 R^m(\boldsymbol{k}_\parallel))$$
$$- \frac{1}{N}\sum_{q_\parallel} A^{\mathrm{p}}(2\overline{N}_{q_\parallel} + 1) - B^{\mathrm{p}}(\boldsymbol{k}_\parallel)\langle Q(\boldsymbol{k}_\parallel)\rangle\delta_{k0}, \tag{11}$$

with $\overline{N}_{q_\parallel} = \langle a_{q_\parallel}^+ a_{q_\parallel}\rangle$ and $\langle Q(\boldsymbol{k}_\parallel)\rangle = \langle a_{k_\parallel}^+ + a_{-k_\parallel}\rangle$. Due to the coupling of the phonons to the electric as well as to the magnetic subsystem the phonon excitation energy is characterized by the polarization P, the magnetization M and the spin–phonon coupling parameters R^e and R^m, too.

The polarization and the magnetization are calculated self-consistently from the corresponding Green's functions for the ferroelectric and magnetic subsystem. In the same manner as the dispersion relation of the phonon system we get also the damping of the phonons using the method proposed in Ref. [21].

4 Results

Now let us present the numerical results based on our analytical findings. To do that the following model parameters, appropriate for BMNO, are used $T_{\mathrm{N}}^{(b)} = 140\,\mathrm{K}$ and $T_{\mathrm{c}}^{(b)} = 485\,\mathrm{K}$, $A^{(b)} = 58\,\mathrm{K}$, $J^{(b)} = 310\,\mathrm{K}$, $\Omega^{(b)} = 2\,\mathrm{K}$, $g^{(b)} = 50\,\mathrm{K}$, $F^{e(b)} = F^{m(b)} = 6\,\mathrm{cm}^{-1}$, $R^{m(b)} = -10\,\mathrm{cm}^{-1}$, $R^{e(b)} = -50\,\mathrm{cm}^{-1}$, $A^{\mathrm{p}(b)} = -5\,\mathrm{cm}^{-1}$, $B^{\mathrm{p}(b)} = 0.5\,\mathrm{cm}^{-1}$, $\omega_0 = 610\,\mathrm{cm}^{-1}$, and $S = 1$ for the Ni-ions and $S = 3/2$ for the Mn-ions. As mentioned before the superscript (b) is related to the bulk material, whereas (s) characterizes the surface. For simplicity we assume nearest-neighbor exchange interaction and take $J_{ij} = J^{(s)}$, $A_{ij} = A^{(s)}$, $R^{(s)}$ on the surface of the thin film and $J_{ij} = J^{(b)}$, $A_{ij} = A^{(b)}$, $R^{(b)}$ in the bulk. They can be enhanced or reduced compared to the bulk values. Because the anharmonic spin–phonon interaction parameters R^e or R^m are related to the second derivative of J_{ij} or A_{ij} [22] it results also a change of the spin–phonon coupling on the surface.

Let us comment the origin of the parameters used here. The exchange interaction constants are calculated from their relation to the critical temperatures. The magnetoelectric coupling constant g is obtained indirectly from the expression for the exchange coupling A_{ij} and J_{ij} after calculation of the renormalized exchange interaction constants. The phonon–phonon interaction parameters follow from fitting the experimental data above the critical temperatures where the spin–phonon interactions vanish. The spin–phonon interaction constants are obtained from the experimental data at low temperatures, where the phonon–phonon interactions play only a minor role.

In Fig. 1 the temperature dependence of the phonon energy of a BNMO thin film with $N = 7$ layers is shown. The phonon energy decreases with an increase of the temperature T. Such a softening is reported for BNMO thin films in [10] and BFCO thin films [11]. Below the magnetic transition T_{N} the system exhibits magnetic and ferroelectric properties. Fig. 1, curve 1, illustrates clearly the coupling between the electric and magnetic properties below T_{N}, which is manifested as a kink at the magnetic phase transition temperature $T_{\mathrm{N}} = 123\,K$. This anomaly can be explained as an influence of vanishing magnetic ordering on the structural and the electric ordering in the system. Because of $T_{\mathrm{N}} \ll T_{\mathrm{c}}$, the magnetic system cannot influence the electric one above T_{N}, the two phases coexist only below T_{N}. A similar small kink in the dielectric constant is observed in BNMO thin films in Ref. [2] indicating the interplay between ferromagnetic and ferroelectric interactions. The anomaly is attributed also to the strong anharmonic spin–phonon coupling characterized by the coupling R^m. In case $R^m = 0$ the kink disappears. Generally the kink can be considered as

Original

Paper

Phys. Status Solidi B 249, No. 8 (2012)

1605
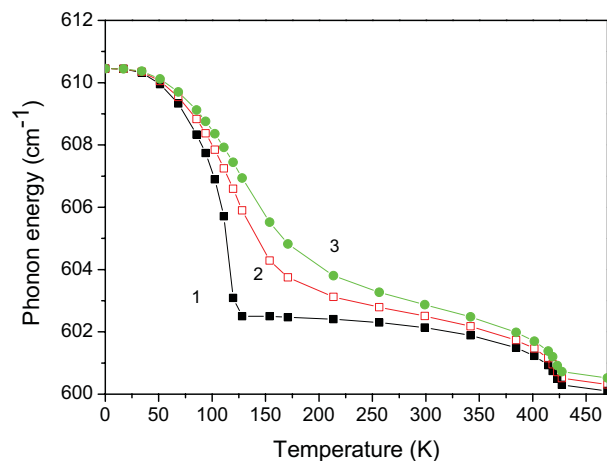
Figure 1 (online color at: www.pss-b.com) Temperature dependence of the phonon energy in BMNO thin films with $A^{(s)} = 52\,K$, $J^{(s)} = 290\,K$, $R^{m(s)} = -8\,cm^{-1}$, and $R^{e(s)} = -45\,cm^{-1}$ for $h = 0$ (1), 10 (2), and 20 K (3).

an evidence that the spin–lattice coupling is modified due to the magnetoelectric effect. Obviously the magnetic exchange energy is enhanced when the magnetic ions shift their positions. This effect is particularly strong near to or below the magnetic phase transition and may result in structural anomalies and a change of the dielectric properties. A smaller kink is observed at the Curie temperature T_c due to anharmonic pseudo-spin–phonon interaction characterized by the coupling R^e. In the same manner one gets a softening of the phonon mode in BNMO near T_c. Above T_c the pseudo-spin–phonon interaction disappears and consequently only the anharmonic phonon–phonon interaction remains. In that case the phonon mode decreases very slowly and it is nearly temperature independent.

The phonon damping γ, related to the width of the Raman peaks, increases with increasing temperature.
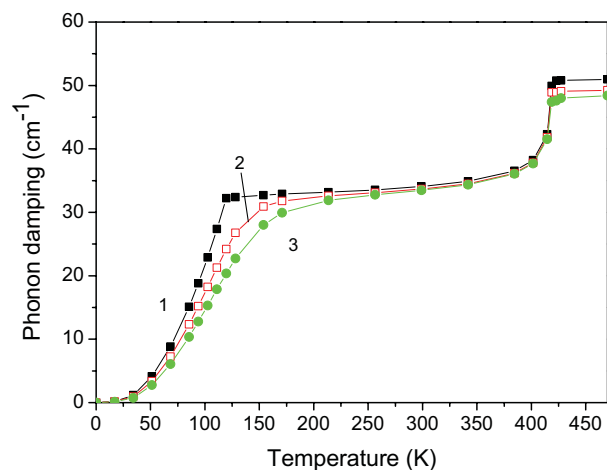
Figure 2 (online color at: www.pss-b.com) Temperature dependence of the phonon damping in BMNO thin films with $A^{(s)} = 52\,K$, $J^{(s)} = 290\,K$, $R^{m(s)} = -8\,cm^{-1}$, and $R^{e(s)} = -45\,cm^{-1}$ for $h = 0$ (1), 10 (2), and 20 K (3).
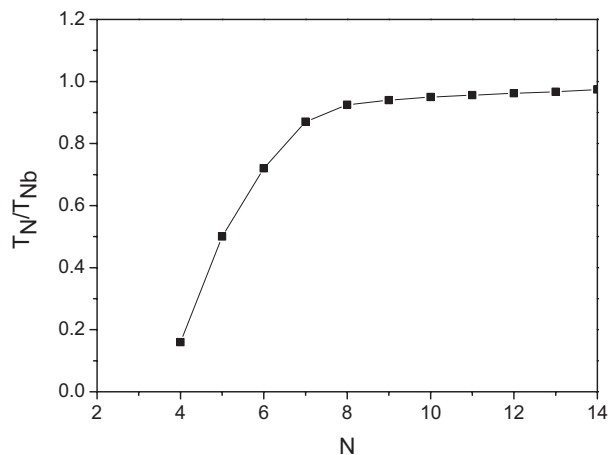
Figure 3 Thickness dependence of the magnetic phase transition temperature T_N in BNMO thin films.

Around the magnetic transition temperature $T_N = 123\,K$ one observes again a kink in γ, see Fig. 2 (curve 1). The damping grows up in case the anharmonic spin–phonon interaction constant R^m is enhanced.

A feature of the magnetoelectric effect is the ability to control the system by external electric and magnetic fields. In Figs. 1–2 we demonstrate that the phonon energy increases with an increasing magnetic field whereas the phonon damping decreases with h, see curves 2 and 3.

Both Figs. 1–2 suggest that the critical temperatures T_N and T_c for BNMO thin films are smaller compared to the bulk case. In Fig. 3 we present the thickness dependence of the magnetic phase transition temperature based on our model. The critical temperature decreases with decreasing film thickness. For seven layers the temperature is fixed by $T_N = 123\,K$. A similar decrease of T_N is also reported for BMNO thin films in [2] and for BNMO nanoparticles in Ref. [23] with $T_N = 122\,K$.

In conclusion, the physical properties of multiferroic BMNO thin films are studied based on a microscopic model. In particular, the phonon frequency and its damping is analyzed. The phonon spectrum reveals a kink at the magnetic phase temperature indicating a strong evidence for a magnetoelectric coupling. Furthermore, the phonon mode is controlled by an external magnetic field.

To our understanding the model proposed is also applicable for other materials like Bi2M(1)M(2)O6 ($T_c \gg T_N$), where the two magnetic ions M(1)M(2) could be Fe–Mn, Co–Mn, and Fe–Cr. In case the Yttrium atoms in the compound Y_2MNO is subjected to a distortion similar to the Bi in BMNO we expect that our model is also useful for that material. As far we know an experimental verification for Y_2MNO is still missing. So we would suggest to test the predictions of our model for Y_2MNO.

References

[1] M. Azuma, K. Takata, T. Saito, S. Ishwata, and M. Takano, J. Am. Chem. Soc. **127**, 8889 (2005).

[2] M. Sakai, A. Masumo, D. Kan, M. Hashisaka, K. Takata, M. Azuma, M. Takano, and Y. Shimakawa, Appl. Phys. Lett. **90**, 072903 (2007).

[3] Y. Shimakawa, D. Kan, M. Kawai, M. Sakai, S. Inoue, M. Azuma, S. Kimura, and O. Sakata, Jpn. J. Appl. Phys. **46**, L845 (2007).

[4] P. Padhan, P. LeClair, A. Gupta, and G. Srinivasan, J. Phys.: Condens. Matter **20**, 355003 (2008).

[5] R. Nechache, C. Harnagea, L. P. Carignan, D. Menard, and A. Pignolet, Ferroelectrica **101**, 152 (2008).

[6] R. Nechache, C. Harnagea, L. P. Carignan, D. Menard, and A. Pignolet, Philos. Mag. Lett. **87**, 231 (2007).

[7] R. Nechache, L. P. Carignan, L. Gunawana, G. Harnagea, C. Botton, D. Menard, and A. Pignolet, J. Mater. Res. **22**, 2102 (2007).

[8] A. Ciucivara, B. Sahu, and L. Kleinman, Phys. Rev. B **76**, 064412 (2007).

[9] S. Kumar, G. Giovannetti, J. van den Brink, and S. Picozzi, Phys. Rev. B **82**, 134429 (2010).

[10] M. N. Iliev, P. Padhan, and A. Gupta, Phys. Rev. B **77**, 172303 (2008).

[11] S. Kamba, D. Nuzhnyy, R. Nechache, K. Závěta, D. Nižňanský, E. Šantavá, C. Harnagea, and A. Pignolet, Phys. Rev. B **77**, 104111 (2008).

[12] R. Blinc and B. Zeks, Soft Modes in Ferroelectrics and Antiferroelectrics (North-Holland, Amsterdam, 1974).

[13] R. Pirc and R. Blinc, Phys. Rev. B **70**, 134107 (2004).

[14] X. S. Wang, C. L. Wang, and W. L. Zhong, Solid State Commun. **122**, 311 (2002).

[15] H. X. Cao and Z. Y. Li, J. Phys.: Condens. Matter **15**, 6301 (2003).

[16] N. A. Pertsev, A. K. Tagantsev, and N. Setter, Phys. Rev. B **61**, R825–R829 (2000).

[17] J. M. Wesselinowa and S. Kovachev, J. Appl. Phys. **102**, 043911 (2007).

[18] J. M. Wesselinowa and I. Apostolova, J. Appl. Phys. **104**, 084108 (2008).

[19] J. M. Wesselinowa and I. Georgiev, Phys. Status Solidi B **245**, 1653 (2008).

[20] A. Bhattacharjee, O. Erikson, B. Sanyal, arXiv:1001.0128v2 2010.

[21] Y. Tserkovnikov, Theor. Math. Phys. **7**, 250 (1971).

[22] J. M. Wesselinowa and S. Kovachev, Phys. Rev. B **75**, 045411 (2007).

[23] Y. Du, Z. X. Cheng, X. L. Wang, P. Liu, and S. X. Dou, J. Appl. Phys. **109**, 07B507 (2011).